HIGH QUALITY SURFACE PASSIVATION AND HETEROJUNCTION FABRICATION BY VHF-PECVD DEPOSITION OF AMORPHOUS SILICON ON CRYSTALLINE SI: THEORY AND EXPERIMENTS

Luc Fesquet, Sara Olibet, Evelyne Vallat-Sauvain*, Arvind Shah, Christophe Ballif.

Institute of Microtechnology (IMT), University of Neuchâtel
Rue A.L Breguet, 2, CH 2000 Neuchâtel, Switzerland
* currently at Oerlikon Solar-Lab, Neuchâtel Switzerland

ABSTRACT: Hydrogenated Amorphous Silicon (a-Si:H) deposited by Very High Frequency Plasma Enhanced Chemical Vapor Deposition (VHF PECVD) proves to be very efficient in passivating crystalline silicon surfaces. To characterize these a-Si:H/c-Si structures, the Quasi Steady State (QSSPC) and Photoconductance Decay (PCD) methods are used, giving the effective lifetime and the related effective surface recombination velocity S_{eff} as a function of the excess carrier density (ECD). We show that, both on n- and p-type c-Si, surface recombination velocities (S_{eff}) lower than 10 cm/s are reached using passivating of stacks of intrinsic and doped a-Si:H layers. We show how the S_{eff}=f(ECD) results can be described by a model based on recombination through amphoteric defect states at the a-Si:H/c-Si interface. This model is also used to estimate charges and defect densities obtained by depositing intrinsic and doped layers on p-type c-Si. High efficiency a-Si:H/c-Si heterojunction solar cells are shown to benefit directly from the development of intrinsic and doped layers. Thanks to the excellent surface passivation, high V_{oc}'s are reached, on both p- (690mV) and n-type (713mV) c-Si and a conversion efficiency up to 19.1% is achieved for cells prepared on flat n-type Si wafers. Finally, we show how the dark recombination current density (J_0) of the final solar cell on p- and n-type c-Si wafer is directly related to the value of its V_{oc}, with a common ideality factor n of 1.2 for all devices.
Keywords: Heterojunctions, Passivation, a-SiH.

1 INTRODUCTION

Hydrogenated amorphous silicon (a-Si:H) deposited onto crystalline silicon (c-Si) is of high interest to achieve high efficiency silicon solar cells. Moreover solar cells based on the a-Si:H/c-Si structure are valuable thanks to their low temperature process. The HIT heterojunction solar cells (n-type c-Si) from Sanyo exhibit conversion efficiency up to 21.8% and an open circuit voltage (V_{oc}) of 730mV [1]. Solar cells based on p-type wafers [2] can achieve excellent conversion efficiency and V_{oc}, even though it is still controversial to know if they can reach values obtained on n-type.

When using high lifetime crystalline Si wafer, achieving optimized surface passivation is the main issue. As in this case the bulk recombination is low, defects at the surface become the predominant recombination centers of the charge carriers generated in the bulk. Silicon based nitride (SiN_x) [3] or oxide (SiO_2) [4] are well known for their c-Si surface passivation properties. Amorphous hydrogenated silicon deposited at low temperature by PECVD shows also c-Si passivation assets [5] [6] [7]. The thin a-Si:H layer induces the passivation of the surface dangling bonds by hydrogen contained in the amorphous phase, while, as shown in [6] the state of charge of the amphoteric defects in the a-Si:H/c-Si interface can engender an electric field repelling the charge carriers approaching the surface in the c-Si.

In heterojunction silicon solar cells, the thin intrinsic layers are capped with doped layers. These doped layers influence the field effect passivation. By tuning the intrinsic and doped layers, one can optimize the passivation properties and therefore achieve high conversion efficiency devices, with excellent V_{oc}.

2 c-Si SURFACE PASSIVATION BY a-Si:H

2.1 Theory: Modeling surface passivation

In this part we recall the features of a new model introduced by Olibet et al. [6] to describe the passivation of c-Si by a-Si:H. It can be split in two processes: interface recombination through amphoteric defects and field effect passivation by surface charges.

Surface recombination through hydrogenated amorphous silicon dangling bonds is modeled by reducing the bulk amorphous silicon model by Hubin *et al.*[8] into a 2-D model.

This model considers amphoteric state recombination centers. These centers possibly have three charges: negative, neutral, or positive. Fig.1 shows the two different paths of recombination.

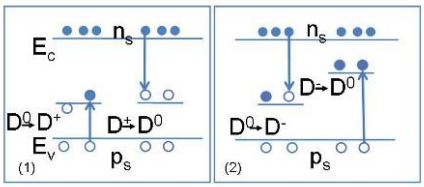

Figure 1 The two possible recombination events in amorphous silicon, through an amphoteric defect D0: on the left, the center in the neutral state captures first a hole, and then captures an electron to become neutral again. On the right, the center in the neutral state captures first an electron and then captures a hole.

The surface recombination rate is calculated using Eq.1, where U_s is the surface recombination rate, n_s and p_s the free carrier densities at the surface, N_s the density of surface dangling bonds and v_{th} the thermal velocity. The capture cross sections of the different recombination processes are important parameters, as they define the dominant recombination path, and thus the average charge of the defects. The best common values for fitting a wide set of experimental data (different layers on all kind of doped wafers) are $\sigma_n^0/\sigma_p^0 = 1/20$ and $\sigma_p^-/\sigma_p^0 = \sigma_n^+/\sigma_n^0 = 500$.

$$U_S = U_{DB} = \frac{n_S\sigma_n^0 + p_S\sigma_p^0}{\frac{p_S}{n_S}\frac{\sigma_p^0}{\sigma_n^+} + 1 + \frac{n_S}{p_S}\frac{\sigma_n^0}{\sigma_p^-}} v_{th} N_S \ [\mathrm{cm^{-2}s^{-1}}] \qquad (1)$$

In order to find n_s and p_s, the surface potential has to be considered. As shown in Fig.2, due to this potential, the energy bands bend near the surface. Thus, free carrier densities at the surface (n_s, p_s) are different from the ones in the bulk (n,p), but are related by Eq.2:

$$n_S = n \cdot exp(q\Psi_S/kT)\ [cm^{-3}]$$
$$p_S = p \cdot exp(-q\Psi_S/kT)\ [cm^{-3}] \quad (2)$$

It is assumed that this surface potential is induced by charges in the thin amorphous film at the a-Si:H/c-Si interface. The density of field effect active charges in the amorphous Q_s, can then be related to the mirrored charge density in the silicon bulk: $Q_s=-Q_{si}$

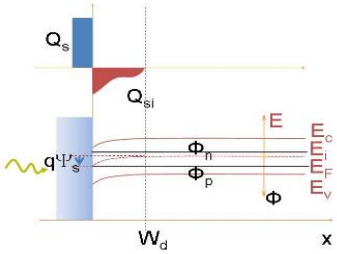

Figure 2 Surface charge density inducing a surface potential and band bending at the c-Si/a:Si:H interface.

With this assumption, Q_s and Ψ_s, and as a result n_s and p_s, are linked by a non linear equation [9].

Knowing U_s, the surface recombination velocity S_{eff}, defined at the edge of the space-charge region, is then accessible through Eq.3.

$$S_{eff} \equiv U_S/\Delta n \ [\text{cm/s}] \quad (3)$$

Where, $\Delta n = \Delta p$ are the free excess carrier densities at the edge of the space charge region. According to this model, in which Q_s and N_s are the two parameters, measured surface recombination velocity as a function of the excess free carrier density can be fitted.

2.2 From effective lifetime to surface recombination velocity

S_{eff} depends on the free excess carrier density (ECD). From its absolute level and its variation we can deduce the surface passivation mechanism of specific passivation layers. However, the surface recombination velocity is not a measureable quantity, but is related to the effective lifetime τ_{eff} by Eq.4:

$$S_{eff} = (1/\tau_{eff} - 1/\tau_b) \cdot W/2 \quad (4)$$

Where τ_b is the bulk lifetime and W the wafer's thickness. τ_{eff} can be measured by different manners. The Sinton Lifetime tester [10] used in this work measures lifetimes by the transient photoconductance decay (PCD) method as well as the quasi steady state PC (QSS PC) method.

These lifetime measurement methods allow the calculation of the open circuit voltage (V_{oc}) as a function of the illumination level, determined by the splitting of the pseudo Fermi level of the electrons (φ_n) and holes (φ_p) in the c-Si (Eq.5).

$$V_{OC} = \phi_p - \phi_n = kT/q \cdot \ln\left(\frac{np}{n_i^2}\right) \quad (5)$$

The 1-sun V_{oc} value is useful, as it provides a preview of final solar cell performance, and thus can be used to monitor the passivation improvement.

3 PASSIVATION EXPERIMENT AND ANALYSIS

To control the passivation quality of the intrinsic and doped layers and also the quality of the surface cleaning process, effective lifetime measurements are of significant help. Using the Sinton lifetime tester, identical a-Si:H layers or stacks of layers have to be deposited on both sides of the crystalline silicon wafer.

3.1 Experimental

The c-Si used in this work are flat, Float Zone boron doped wafers with a resistivity of 2.5Ωcm and a thickness of 300µm. Before a-Si:H deposition, the native oxide is removed in a diluted hydrofluorhydric acid (HF) solution for 45s, dried with nitrogen, and then put in the load lock of the PECVD system as fast as possible. The a-Si:H layers are deposited at 180°C by Very High Frequency (70MHz) PECVD, using a mixture of Silane and Hydrogen. For the doped layers Phosphine (PH_3) and Trimethylborane (TMB) gases diluted in hydrogen are used. The intrinsic silicon is deposited at a hydrogen dilution of 2.5, a pressure of 0.4mbar and a power of 20mW/cm^2. For phosphorus microdoped (n-µdoped) layers some ppms of phosphine are added. After deposition, samples are annealed at 180°C during 180 minutes. Four different a-Si:H passivating layers are deposited. The first one consists of a 50 nm of intrinsic a-Si:H, and it is used as a test. As it has good passivating property, and no charge that could passivate the c-Si surface by field effect, its use is a good mean to control the wafer surface, the HF bath and the PECVD system cleanliness. The second layer is made of 50nm of phosphorus µdoped a-Si:H. The other two passivating layers are to form a future heterojunction: 5nm of intrinsic a-Si:H and 20nm of p doped a-Si:H for the first of them, and 5 nm µdoped a-Si:H and 25nm of n doped a-Si:H for the second one.

3.2 Surface recombination velocity

The effective lifetime as a function of the ECD for these symmetric passivations is measured by QSSPC and the corresponding effective surface recombination velocity is calculated, assuming that the bulk lifetime τ_b is 5ms. The results in Fig.3 show that an effective lifetime of 1.6ms is reached with the i/p layer passivation, resulting in S_{eff} as low as 6cm/s. S_{eff} of n-µdoped/n layer is down to almost 20cm/s. The 50nm n-µdoped layer surface recombination velocity curve is in-between the 2 doped layers. In the case of the 50nm thick intrinsic layer, S_{eff} as good as for i/p layers is obtained at high injection levels, but at low injections, S_{eff} is higher than in all the other cases.

These curves can be fitted using the recombination through amphoteric states model. The fit curves are represented by full lines on the graph. The values of the

parameters N_s and Q_s found to fit best to the experimental curves are summarized in table 1. It can be seen that for the 50 nm intrinsic a-Si:H layer both Qs and Ns are low. In n-µdoped layers, the phosphorus increases the defect density at the a-Si:H/c-Si interface, and therefore Ns. At the same time the number of the negatively charged dangling bonds induced by the phosphorus doping, and so on Qs, is 10 times higher.

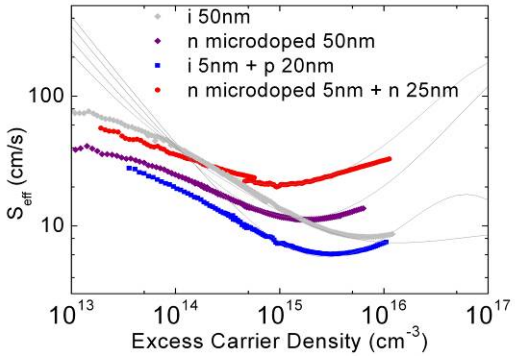

Figure 3 Surface recombination velocities of intrinsic, n-µdoped and stacked i/p, n-µdoped /n layers on p c-Si 2.5 Ωcm.

The i/p layer benefits from the good quality of the i a-Si:H, while the p layer engenders large amount of positive charges. Finally, the n-µdoped/n layer shows, as for n-µdoped layer, a charging effect and, at the same time, an increase of the surface defect density. As it can be seen, a field effect induced by interface charges is of high interest for the passivation, since, with a similar value of defect density, the charged i/p layer shows a significantly lower surface recombination velocity as compared to the intrinsic, lightly charged layer. However, it can be seen that layers or stacked layers containing phosphorus induce a higher surface defect density on this 2.5Ωcm p-type c-Si than i or stacked i/p layers.

Table 1 Fitted Surface defect density and surface charge density of a-Si:H layers on a 2.5Ωcm FZ p-type c-Si wafer.

Sample	Ns ($10^9 cm^{-2}$)	Qs ($10^{10} cm^{-2}$)
i 50 nm	**5.2**	**-7**
n-µdoped 50 nm	**53**	**-85**
i 5 nm + p 20nm	**3.2**	**150**
n-µdoped 5 nm + n 25nm	**40**	**-50**

As an implied V_{oc} of the device can be determined using Eq.5, the effect of the different layers on this parameter are directly accessible.

Thus, these passivation tests serve to develop the intrinsic and doped layers that will afterward be used in the final solar cells. Implied V_{oc} values of the symmetrical i/p and n-µdoped/n stacked layers are 720mV resp. 680mV. In an asymmetrical structure, this last layer will thus be the predominant recombining interface.

4 SOLAR CELL HETEROJUNCTIONS

4.1 Experimental

The final solar cell devices are made in the same conditions as the passivating layers previously studied i.e. on one side an i/n layer is formed, then the wafer is turned and then the i/p layer is deposited. Subsequently, DC sputtered ITO is used to form the front and back contacts. Finally on the back contact Aluminium or Silver are deposited by DC sputtering.

To characterize the effective lifetime of this asymmetric passivation, samples are cut in two pieces after the a-Si:H layer deposition. One, named precursor, is dedicated to lifetime measurements, and the other one is front and back contacted.

Measurements made on the contacted solar cells are current-voltage in dark and under illumination, Suns-V_{oc} and external quantum efficiency to extract the short circuit-current density.

4.2 From passivating layers to final solar cell

Using the previous i/p and n-µdoped/n layers solar cell heterojunctions were made.

Lifetime measurements (Fig.4) on the solar cell precursor show good surface passivation yielding a maximal lifetime as high as 0.4 ms. The predicted V_{oc} of this sample is about 675mV, and as expected is closed to the implied V_{oc} of the symmetrical n-µdoped/n layers. IV measurements of the final cells indicated a similar V_{oc} of 677mV. This comparison between implied and real V_{oc} shows that the ITO and metal depositions do not affect the passivation performance of the a-Si:H layers. Suns-V_{oc} measurements of finished solar cells provide a similar observation, and on a wider ECD range. Using Eq.5, the variation of the effective lifetime as a function of the ECD can be deduced from this measure.

Fig.4 shows a good superimposition of the lifetime measured by QSSPC on the precursor (green curve) and by Suns-V_{oc} on the final device (blue curve) which is verified in most of the ECD range.

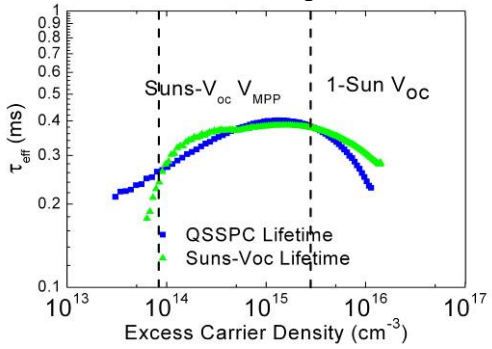

Figure 4 Effective carrier lifetime as a function of ECD of the solar cell precursor on p type c-Si. Dashed lines define the V_{oc} and the V_{MPP} of the Suns-V_{oc} Curve.

The highest V_{oc}, obtained on a flat p-type wafer, is 690mV on 0.5Ωcm, which makes it possible to reach a conversion efficiency as high as 16.5%.

4.3 High efficiency solar cells on n and p-type wafer

Table 2 Best V_{oc} and efficiency values on n- and p-type wafers.

Wafer Type	V_{oc}(mV)	FF	Eff (%)
n phosporus 1Ωcm	713	74	16.9
n phosporus 1Ωcm	682	82	19.1
p boron 0.5Ωcm	690	74	16.3

Table 2 summarizes our best results obtained up to now on p- and n-type flat wafers. Heterojunction solar cells based on n-type c-Si achieve the best conversion efficiency until now. On n-type c-Si, the highest conversion efficiency obtained is 19.1 % with a V_{oc} of 682mV and a Fill Factor (FF) of 82%, on 1Ωcm flat wafer. On n-type, the achieved efficiency is higher than on p-type, but the V_{oc} values are on both cases high. One hypothesis made to understand this efficiency discrepancy is non optimum valence and conduction band offsets repartition [11].

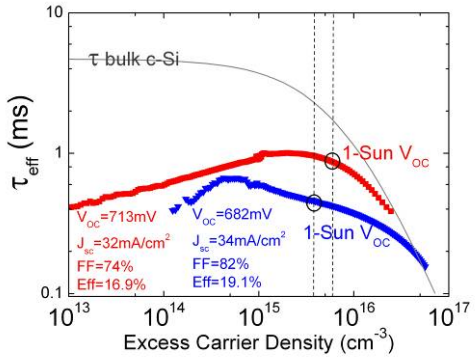

Figure 5 Effective lifetime and surface recombination velocity of the best V_{oc} and best efficiency solar cells on 1 Ωcm c-Si.

Lifetime measurements of the best efficiency solar cell precursor presented on Fig.5 exhibit low surface recombination and hence high V_{oc}. τ_{eff} higher than 0.6ms is reached in this case. The V_{oc} value implied is 685mV, close to the real value. The solar cell with the best V_{oc} of 713mV has an τ_{eff} higher than 1ms, and an implied V_{oc} of 708mV.

From our best results, plotted on Fig.6, it is clearly visible that there is a trade-off between high V_{oc} and high FF.

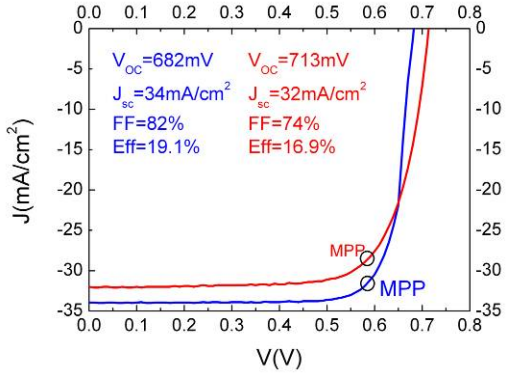

Figure 6 Current-Voltage curves of the highest-V_{oc} and best efficient solar cells on n-type c-Si.

High V_{oc} values can be attained with thicker layers, but as a consequence, lower short circuit current (J_{sc}) due to absorption in non-active layers and lower FF are obtained. For the solar cell optimization, symmetrical passivation structures evaluated by lifetime measurements allow a faster development of stacks of a-Si:H layers that have the required qualities.

4.4 Relation between dark IV parameters and V_{oc}

Lifetime and Suns-V_{oc} measurements are effective to define and optimize some key parameters of the solar cells (effective lifetime, 1-sun V_{oc}). However these measurements are done in V_{oc} condition. To improve the comprehension of the device, it is interesting to investigate the link between the 1-sun V_{oc} (and then the lifetime) of a cell to dark IV characteristics. Under illumination, the current density as a function of the voltage can be expressed as Eq 6:

$$\boldsymbol{J = J_0\left[\exp\left(\frac{qV}{nkT}\right)-1\right]-J_{ph}} \qquad (6)$$

Where J_0 is the saturation current density, n the diode ideality factor, q the electron charge, k the Boltzmann's constant, and J_{ph} the photogenerated current. This expression is valid when the diffusion current is much higher than the recombination current, i.e. 0.4<V<0.7. In the dark (J_{ph} =0) the relation between J and V only depends on n and J_0.

The heterojunction solar cells dark IV curves are, in this specific voltage range, well characterized by this model and interesting observations can be drawn by analyzing the J_0, n value sets. From the measurements on various c-Si substrate resistivities (n- and p-types) and a-Si:H stacked layers, the diode ideality factor appears to stay constant at 1.2, whereas J_0 varies.

Under illumination, in the case of J=0, V=V_{oc}, Eq.6 can be formulated as:

$$\boldsymbol{V_{oc} = \ln\left(\frac{J_{ph}}{J_0}\right)\times\frac{nkT}{q}} \qquad (7)$$

Then the plot of the 1-Sun V_{oc} as a function of $\ln(J_0)$ should exhibits a slope corresponding to q/nkT if n is constant, which is indeed observed in Fig.7.

Fujiwara *et al.* [12] found a similar trend between J_0 and 1-Sun V_{oc}, reporting a value of 1.24 for n for their best V_{oc} solar cell, also in accordance with Sanyo's values [13], all for n-type wafers,. Thus our results are in good agreement with these previous works and values obtained for high quality devices. Furthermore, it is shown here that this tendency can be generalized for p-type c-Si heterojunctions.

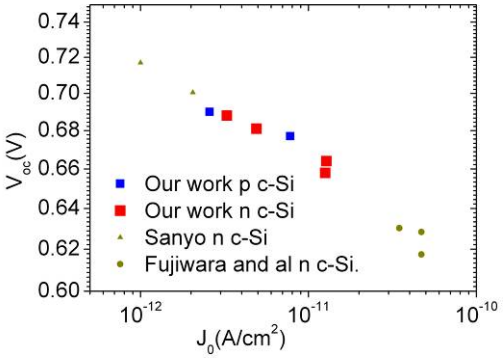

Figure 7 V_{oc} of various heterojunctions solar cells as a function of the saturation current density. Heterojunctions from Fujiwara *et al.* are single side heterojunctions with a recombining Aluminum contact.

These results prove that a 1 diode equation defines well the solar cell behavior, at less near the 1-Sun V_{oc}.

Moreover, it has been seen that the V_{oc} is linked to the a-Si:H/c-Si interface passivation property. Thus, for the various c-Si based solar cells analyzed, J_0 measurement can be a control tool of the passivation property. In a reciprocal way, this means that not only implied V_{oc}, but also J_0, can be deduced accurately from lifetime measurement.

5 CONCLUSION

Excellent surface passivation of crystalline silicon can be achieved using high quality intrinsic and doped layers of VHF-PECVD grown hydrogenated amorphous silicon (a-Si:H). The surface recombination model based on amphoteric defects at the a-Si:H/c-Si interface reproduces the experimental effective surface recombination velocity (S_{eff}) as a function of the excess carrier density measured by QSSPCD and transient methods. The parameters used for the fit are the surface charge density (Q_s) and the defect density (N_s) at the interface between c-Si and a-Si:H. In order to attain very low S_{eff}, the parameters N_s and Q_s need to be combined. Best passivation results were obtained by associating low N_s which reduce the probability for the charge carrier at the interface to recombine, and high Q_s which create an electric field that keeps away recombination partners from bulk c-Si. a-Si:H layers deposited symmetrically on both sides of a c-Si wafer are successfully characterized applying this model.

Final solar cells benefit from this passivation studies and layer development, and high V_{oc} are reached in both p-type (690mV) and n-type (713mV) wafers. The best conversion efficiencies achieved are 19.1% for n-type and 16.3% for p-type c-Si, both on wafer without texturation.

Finally, a logarithmic correlation is found between the saturation current density J_0 and V_{oc} of heterojunction solar cells, on both p-type and n type c-Si, while the diode ideality factor is constant for these devices at a value of 1.2.

Acknowledgments

This work is supported by the Swiss National Science Foundation (FN-200021-107469) and by the Axpo Naturstrom Fonds.

References

[1] E. Maruyama, A. Terakawa, M. Taguchi, Y. Yoshimine, D. Ide, T. Baba, M. Shima, H. Sakata, M. Tanaka, *Proceedings of the 4th IEEE World Conference on Photovoltaic Energy Conversion*, Hawaii, 2006, p. 1455.

[2]T.H. Wang, E. Iwaniczko, M.R. Page, Qi Wang, Y. Xu, Y. Yan, D. Levi, L. Roybal, R. Bauer, H.M. Branz*Proceedings of the 4th IEEE World Conference on Photovoltaic Energy Conversion*, Hawaii, 2006, p. 1439.

[3] M. J. Kerr, A. Cuevas, *Semicond. Sci. Technol.*, **17** (2002) 35.

[4] J. Schmidt and A. G. Aberle, J. Appl. Phys. 85, 3626 (1999).

[5] J. I. Pankove, M. L. Tarng, *Appl. Phys. Lett.*, **34** (1979) 156.

[6] S. Olibet, E. Vallat-Sauvain, C. Ballif, *Phys. Rev. B* **76** (2007) 35326.

[7] S. Dauwe, J. Schmidt, R Hezel, *Proceedings of the 29th IEEE Photovoltaic Specialists Conference*, New Orleans, 2002, p.1246.

[8] J. Hubin, A. V. Shah, E. Sauvain, *Philos. Mag. Lett.*, **66** (1992) 115.

[9] R. Girisch, R. Mertens, R. De Keersmaecker, *IEEE Transactions on electron devices* **35** (1988) 203.

[10] R.A. Sinton and A. Cuevas, Contactless determination of current-voltage characteristics and minority-carrier lifetimes in semiconductors from quasi-steady-state photoconductance data, *Appl. Phys. Lett.*, **69**, (1996) 2510.

[11] N. Jensen, R. M. Hauser, R. B. Bergmann, J.H.Werner, U. Rau, *Prog. Photovolt: Res. Appl.*, 10 (2002) 1.

[12] H. Fujiwara, M. Kondo, *J. Appl. Phys.***101** (2007) 54516.

[13] M. Taguchi, A. Terakawa, E. Maruyama, M. Tanaka, *Prog. Photovoltaics* **13** (2005) 481.